

Morphing from the TV-Norm to the l_0 -Norm

Gengsheng L Zeng^{1*} and Ya Li²

¹Department of Computer Science, Department of Radiology and Imaging Sciences, Utah Valley University, USA

²Department of Mathematics, Utah Valley University, USA

*Corresponding author: Gengsheng L Zeng, Department of Computer Science, Department of Radiology and Imaging Sciences, Utah Valley University, Orem, Lake City, UT 84058 USA

ARTICLE INFO

Received: February 07, 2024

Published: February 21, 2024

Citation: Gengsheng L Zeng and Ya Li. Morphing from the TV-Norm to the l_0 -Norm. Biomed J Sci & Tech Res 55(2)-2024. BJSTR. MS.ID.008665.

ABSTRACT

For piecewise constant objects, the images can be reconstructed with under-sampled measurements. The gradient image of a piecewise image is sparse. If a sparse solution is a desired solution, an l_0 -norm minimization method is effective to solve an under-determined system. However, the l_0 -norm is not differentiable, and it is not straightforward to minimize an l_0 -norm. This paper suggests a function that is like the l_0 -norm function, and we refer to this function as meta l_0 -norm. The subdifferential of the meta l_0 -norm has a simple explicit expression. Thus, it is straightforward to derive a gradient descent algorithm to enforce the sparseness in the solution. In fact, the proposed meta norm is a transition that varies between the TV-norm and the l_0 -norm. As an application, this paper uses the proposed meta l_0 -norm for few-view tomography. Computer simulation results indicate that the proposed meta l_0 -norm effectively guides the image reconstruction algorithm to a piecewise constant solution. It is not clear whether the TV-norm or the l_0 -norm is more effective in producing a sparse solution. Index Terms—Inverse problem, optimization, total-variation minimization, l_0 -norm minimization, few-view tomography, iterative algorithm, image reconstruction

Abbreviations: SSIM: Studies with Structure Similarity; PSNR: Peak Signal-to-Noise Ratio; SNR: Signal-to-Noise Ratio; MLEM: Maximum-Likelihood Expectation-Maximization; POCS: Projections onto Convex Sets

Introduction

COMPRESSED sensing is a technology to use under-sampled measurements for solving an inverse problem [1-4]. When the measurements are insufficient, the imaging system is underdetermined, and the object to be imaged is not well defined. Extra information is required for a useful reconstructed image. For certain objects, extra information is available. The sparseness of an object is an important piece of information. An image array is said to be sparse if most of the array elements are zero. For example, the edge image of a piecewise constant image is sparse. Let us consider the following situation. The desired solution, X , of an inverse problem is sparse after a certain sparsifying transformation ψ , that is, $\psi(X)$ is sparse. The sparseness is measured by the l_0 norm, $\| \cdot \|_0$. If X is a vector,

$$\| x \|_0 \triangleq \text{the total number of nonzero elements in } X. \quad (1)$$

If X is a scalar, $\|X\|_0$ is a binary number as

$$\|x\|_0 \triangleq \begin{cases} 0, & \text{if } x = 0 \\ 1, & \text{if } x \neq 0 \end{cases} \quad (2)$$

An under-determined inverse problem has infinitely many solutions. A compressed sensing solution is a solution with a minimum $\| \psi(X) \|_0$ value.

Mathematically speaking, the l_0 norm is not really a norm nor even a pseudo-norm, because, in general,

$$\| cX \|_0 \neq |c| \cdot \| X \|_0 \quad (3)$$

In this paper, we use the term 'norm' loosely. The difficulty of using the l_0 -norm is that the l_0 -norm is nondifferentiable. Many researchers have attempted to tackle the l_0 -norm minimization problem. The work in [5] converted the l_0 -norm minimization problem into an unconstrained augment Lagrange problem. The work in [6] solved the l_0 -norm minimization problem by introducing auxiliary variables. The l_0 -norm minimization solution used in [7] involved a hard threshold-

ing, linearization, and proximal points techniques. The l_0 -norm minimization is usually achieved by solving some sub problems [8]. Due to the difficulty in minimizing the l_0 -norm, the total variation (TV) norm minimization, which is the l_1 -norm of the gradient, has been given more attention [9-11]. This is because the implementation of the l_1 -norm optimization is much easier than the l_0 -norm optimization. The main purpose of this current paper is to present a simple way to implement the l_0 -norm optimization.

Methods

The l_0 -Norm and Proposed Meta l_0 -Norm

In our two-dimensional (2D) image reconstruction applications, we choose the finite differences in the row and column directions as the sparsifying transformation ψ . Let the 2D image be X and its pixels be denoted as $x_{i,j}$, where i is the row index and j is the column index. At each pixel, $\psi(x_{i,j})$ is a finite difference gradient, which is a 2D vector

$$\psi(x_{i,j}) \triangleq \begin{bmatrix} x_{i+1,j} - x_{i,j} \\ x_{i,j+1} - x_{i,j} \end{bmatrix} \tag{4}$$

The optimization metric (i.e., the objective function) can be set up as the sum of the l_0 -norm of all pixels in the image as

$$M(X) = \sum_i \sum_j \left\| \begin{bmatrix} x_{i+1,j} - x_{i,j} \\ x_{i,j+1} - x_{i,j} \end{bmatrix} \right\|_0 \tag{5}$$

One difficulty of minimizing (5) is that the l_0 -norm is not differentiable and is not easy to optimize. One common method to mitigate the difficulty is to use the l_1 -norm approximation [9-13]. The famous total variation (TV) method is to use the l_1 -norm of the finite difference gradient to replace the l_0 -norm of the finite difference gradient. For a 2D image X , the isotropic TV norm is defined as

$$\begin{aligned} TV_{iso}(X) &= \sum_i \sum_j \left\| \begin{bmatrix} x_{i+1,j} - x_{i,j} \\ x_{i,j+1} - x_{i,j} \end{bmatrix} \right\|_1 \\ &= \sum_i \sum_j \sqrt{(x_{i+1,j} - x_{i,j})^2 + (x_{i,j+1} - x_{i,j})^2}, \end{aligned} \tag{6}$$

and the anisotropic TV norm is defined as

$$TV_{aniso}(X) = \sum_i \sum_j (|x_{i+1,j} - x_{i,j}| + |x_{i,j+1} - x_{i,j}|), \tag{7}$$

This paper proposes an alternative ‘norm’ to replace the l_0 -norm. We refer to the proposed ‘norm’ as the meta l_0 -norm, which is defined for a scalar X as

$$\|X\|_{meta0} \triangleq 1 - e^{-a|X|}, \tag{8}$$

where $0 < a < \infty$ is user-defined parameter. When $X = 0$, $\|X\|_{meta0} = \|X\|_0 = 0$. When $X \neq 0$, $\|X\|_{meta0} \approx \|X\|_0 = 1$ if a is chosen large enough. Figure 1 illustrates the approximation of $\|X\|_0$ by proposed $\|X\|_{meta0}$.

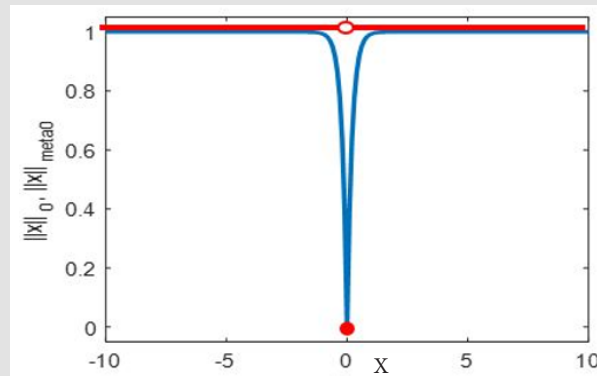


Figure 1: (Blue) $\|X\|_{meta0}$ with $a = 5$; (Red) $\|X\|_0$.

For a 2D vector $X = \begin{bmatrix} x_1 \\ x_2 \end{bmatrix}$ we define the anisotropic meta l_0 -norm as

$$\left\| \begin{bmatrix} x_1 \\ x_2 \end{bmatrix} \right\|_{anisoMeta} \triangleq 1 - e^{-a(|x_1| + |x_2|)}, \tag{9}$$

and define the isotropic meta l_0 -norm as

$$\left\| \begin{bmatrix} x_1 \\ x_2 \end{bmatrix} \right\|_{isoMeta} \triangleq 1 - e^{-a\sqrt{x_1^2 + x_2^2}}. \tag{10}$$

For a 2D image X, we replace (5) by the anisotropic metric

$$M_{\text{anisoMeta}}(X) = \sum_i \sum_j \left[1 - e^{-a(|x_{i+1,j} - x_{i,j}| + |x_{i,j+1} - x_{i,j}|)} \right], \quad (11)$$

or the isotropic metric

$$M_{\text{isoMeta}}(X) = \sum_i \sum_j \left[1 - e^{-a\sqrt{(x_{i+1,j} - x_{i,j})^2 + (x_{i,j+1} - x_{i,j})^2}} \right]. \quad (12)$$

The subdifferential exists for the proposed metric (11) as

$$\begin{aligned} \frac{\partial M_{\text{anisoMeta}}(X)}{\partial x_{i,j}} &= -a \times e^{-a(|x_{i+1,j} - x_{i,j}| + |x_{i,j+1} - x_{i,j}|)} \\ &\times \left[\text{sgn}(x_{i+1,j} - x_{i,j}) + \text{sgn}(x_{i,j+1} - x_{i,j}) \right], \quad (13) \\ &+ a \times e^{-a(|x_{i,j} - x_{i-1,j}| + |x_{i-1,j+1} - x_{i-1,j}|)} \times \text{sgn}(x_{i,j} - x_{i-1,j}) \\ &+ a \times e^{-a(|x_{i+1,j-1} - x_{i,j-1}| + |x_{i,j} - x_{i,j-1}|)} \times \text{sgn}(x_{i,j} - x_{i,j-1}) \end{aligned}$$

where the sign function in (13) is defined as

$$\text{sgn}(x) = \begin{cases} 1, & \text{if } x > 0 \\ 0, & \text{if } x = 0 \\ -1, & \text{if } x < 0 \end{cases} \quad (14)$$

The subdifferential given in (13) readily leads to a gradient descent algorithm to minimize the metric given in (11). The subdifferential for (12) can be similarly obtained.

Application: Few-View Tomography

Here we consider a 2D parallel-beam imaging system, where the image array was 256×256 , the detector contained 256 bins, and the number of views over 180° was 30. The noiseless projection line integrals were generated analytically (without using pixels). A method based on ‘projections onto convex sets’ (POCS) was selected to reconstruct the image. This method alternated between the maximum-likelihood expectation-maximization (MLEM) image reconstruction algorithm and a gradient descent algorithm that minimized the metric $M_{\text{anisoMeta}}(X)$ or $M_{\text{isoMeta}}(X)$. There were 200 iterations used in the POCS algorithm. At each POCS iteration, there were 5000 iterations for the gradient descent algorithm. A flow chart of the algorithm is illustrated in Figure 2. In the computer simulations, the Shepp-Logan phantom was used [14]. In addition to the noiseless data set, a noisy data set was also generated with the zero-mean Gaussian noise added.

In Figure 2, the image reconstruction algorithm ① is the MLEM algorithm:

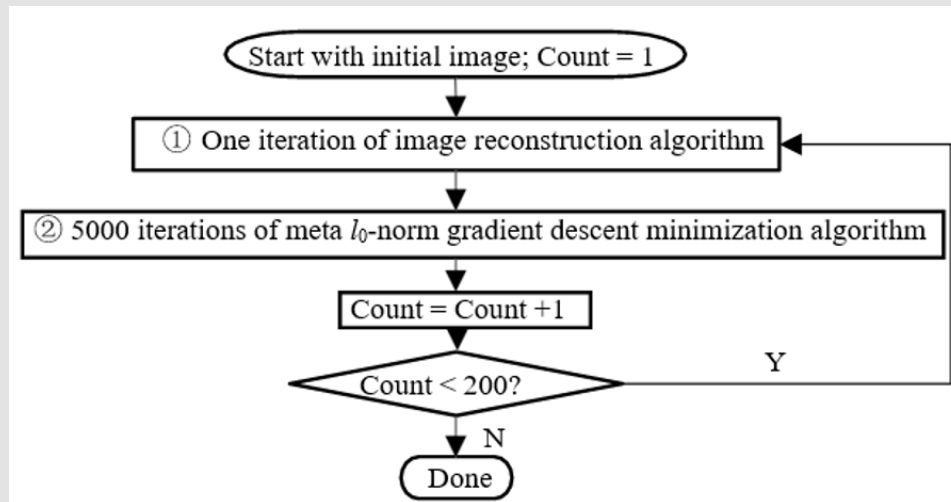


Figure 2: A flowchart of the algorithm used in computer simulations.

$$x_{i,j}^{(k+1)} = \frac{x_{i,j}^{(k)}}{\sum_m a_{i,j,m}} \sum_m a_{i,j,m} \frac{p_m}{\sum_{i,j} a_{i,j,m} x_{i,j}^{(k)}}, \quad (15)$$

where p_m is the m th projection, $a_{i,j,m}$ is the projection contribution from the pixel (i,j) to the projection bin m , and k is the iteration index. In fact, the user can choose any iterative image reconstruction algo-

gorithm for algorithm ①. The gradient descent algorithm ② in Figure 2 is given as

$$x_{i,j}^{(k+1)} = x_{i,j}^{(k)} - \eta \frac{\partial M_{\text{meta}}(X)}{\partial x_{i,j}}, \quad (16)$$

where $\eta = 2 \times 10^{-7}$ in our computer simulations, and $\partial M_{\text{anisoMeta}}(X) / \partial x_{i,j}$ is defined by (13) or $\partial M_{\text{isoMeta}}(X) / \partial x_{i,j}$. The number of iterations

shown in Figure 2 is served as an example only. A TV constrained image reconstruction algorithm was also implemented for the comparison purposes. The TV implementation was in the same format as depicted in Figure 2, except that the gradient $\partial M_{Meta}(X) / \partial x_{i,j}$ was calculated with the TV norm (6) or (7).

Results

The reconstructions via the MLEM, anisotropic/isotropic TV, and the proposed anisotropic/isotropic meta l_0 method are shown in Figures 3 & 4, respectively, for the noiseless and noisy data. Tables 1-4 show the quantitative comparison studies with structure similarity

(SSIM), peak signal-to-noise ratio (PSNR), and signal-to-noise ratio (SNR). When the parameter 'a' is small, the proposed meta l_0 -norms behave like TV norms. On the other hand, when the parameter 'a' is large, the meta l_0 -norms behave like the l_0 -norms. Thus, the proposed meta l_0 -norm are snapshots of the morphing from the TV norm to the l_0 -norm for different 'a' value. When $a = 10000$, the numerical values of the exponential function become underflow. The constraints are not effective and are ignored. It is observed that the l_0 -norm give better SSIM results. However, the TV norms give better PSNR and SNR results. Therefore, we cannot conclude whether the TV norms or the l_0 -norms are the better choices for sparse solutions.

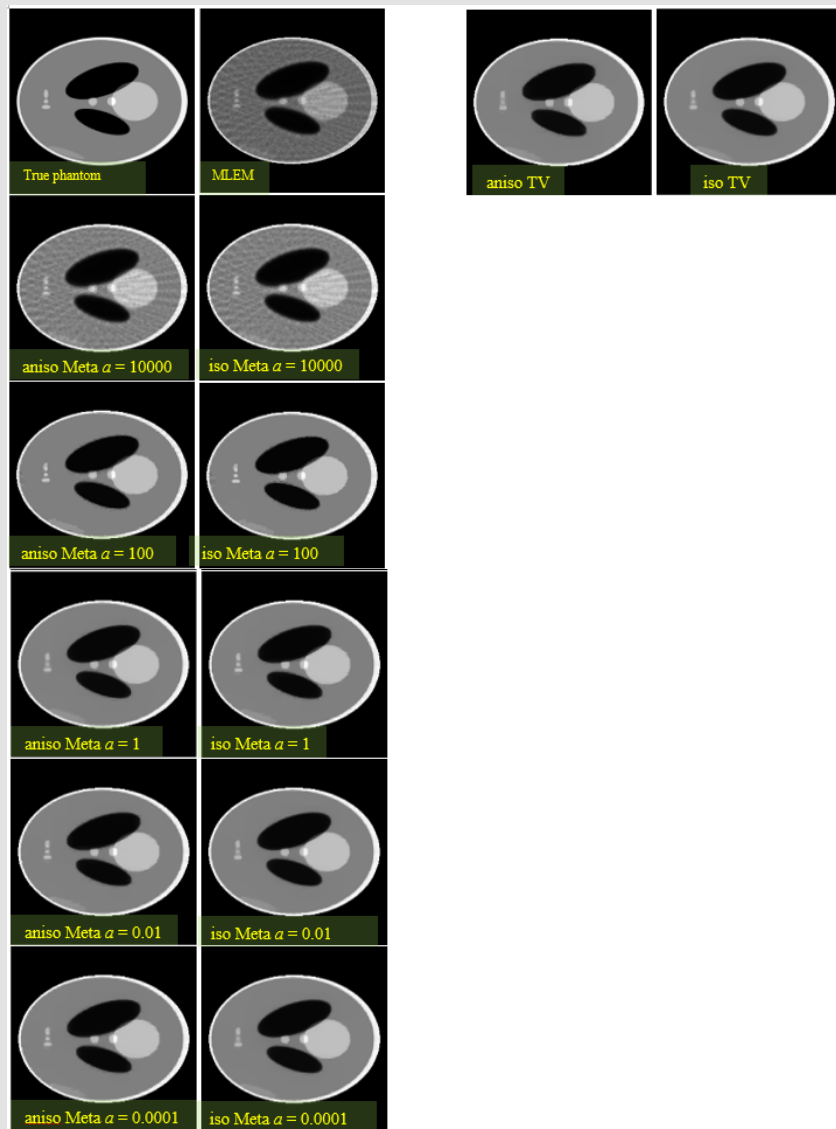


Figure 3: Reconstructions with noiseless data.

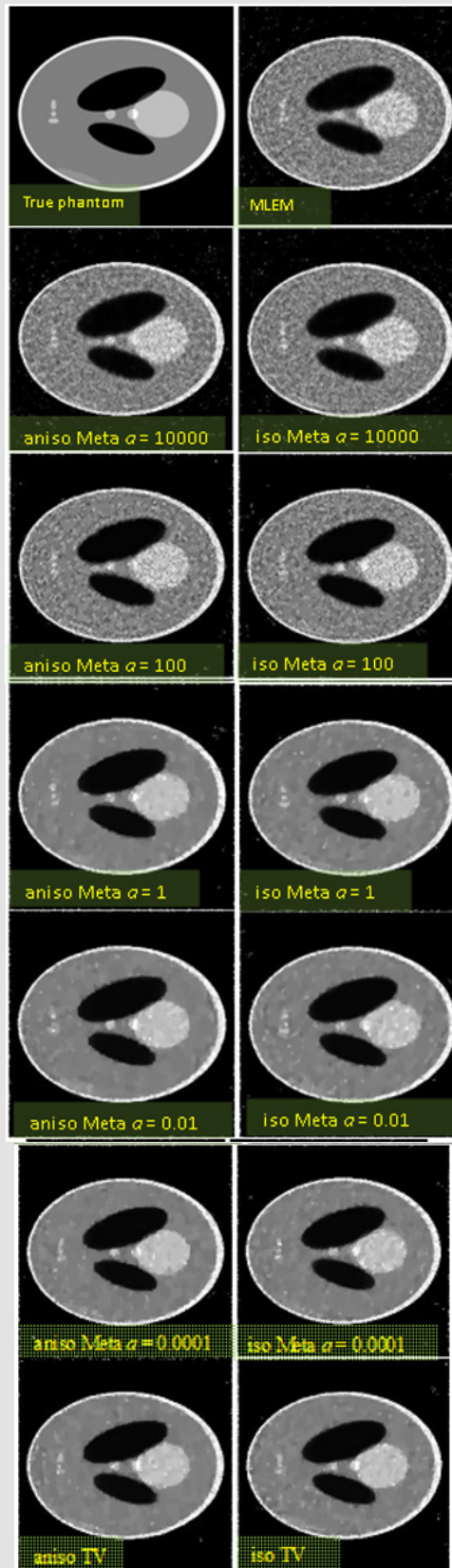


Figure 4: Reconstructions with noisy data.

Table 1: Comparison studies with noiseless data (anisotropic).

Method	SSIM	PSNR	SNR
Ideal case	1	∞	∞
MLEM	0.8771	32.8887	16.5828
anisoMeta $a=10000$	0.8773	32.8935	16.5876
anisoMeta $a=100$	0.9561	34.997	18.6911
anisoMeta $a=1$	0.953	35.9851	19.6792
anisoMeta $a=0.01$	0.9534	36.405	20.099
anisoMeta $a=0.0001$	0.9534	36.4076	20.1016
anisoTV	0.9475	36.9199	20.6139

Table 2: Comparison studies with noiseless data (isotropic).

Method	SSIM	PSNR	SNR
Ideal case	1	∞	∞
MLEM	0.8771	32.8887	16.5828
isoMeta $a=10000$	0.8775	32.8967	16.5908
isoMeta $a=100$	0.9557	34.9854	18.6795
isoMeta $a=1$	0.9509	36.7247	20.4187
isoMeta $a=0.01$	0.9514	37.4011	21.0951
isoMeta $a=0.0001$	0.9514	37.4094	21.1035
isoTV	0.9514	37.4095	21.1035

Table 3: Comparison studies with noisy data (anisotropic).

Method	SSIM	PSNR	SNR
Ideal case	1	∞	∞
MLEM w/ noise	0.6522	28.1125	11.8066
anisoMeta w/ noise, $a=10000$	0.6442	27.889	11.583
anisoMeta w/ noise, $a=100$	0.6932	26.8645	10.5586
anisoMeta w/ noise, $a=1$	0.8642	29.9569	13.6509
anisoMeta w/ noise, $a=0.01$	0.8694	30.7124	14.4064
anisoMeta w/ noise, $a=0.0001$	0.8691	30.6697	14.3638
anisoTV w/ noise	0.8663	30.7298	14.4238

Table 4: Comparison studies with noisy data (isotropic).

Method	SSIM	PSNR	SNR
Ideal case	1	∞	∞
MLEM w/ noise	0.6522	28.1125	11.8066
isoMeta w/ noise, $a=10000$	0.6467	27.9845	11.6785
isoMeta w/ noise, $a=100$	0.686	26.9188	10.6128
isoMeta w/ noise, $a=1$	0.8511	29.8379	13.5319
isoMeta w/ noise, $a=0.01$	0.8605	30.1981	13.8921
isoMeta w/ noise, $a=0.0001$	0.8638	30.3116	14.0056
isoTV w/ noise	0.8625	30.3089	14.0029

Discussion and Conclusions

Simple meta l_0 -norms are suggested in this paper to replace the l_0 -norm in searching a sparse solution for an inverse problem with under-sampled data. These meta norms have a user defined parameter 'a'. The meta l_0 -norms behave like the l_0 -norm when 'a' is large. The most significant advantage of the meta l_0 -norms is that it is sub-differentiable. Therefore, it is straightforward to derive a gradient descent algorithm to minimize the meta l_0 -norms. Computer simulations in this paper show that the meta l_0 -norms are effective in producing a piecewise solution. The meta norms are snapshots between the TV norms and the l_0 -norms. The choice of a better norm is task dependent. The l_0 -norms are not always preferred. We must point out that the l_0 -norm minimization problem is far from being solved. The l_0 -norm minimization problem is NP-hard. The gradient descent algorithm to minimize the meta l_0 -norms is merely a greedy approach. The l_0 -norm minimization problem has multiple minima. Any gradient based methods can only find a local minimum.

References

- DL Donoho (2006) For most large underdetermined systems of linear equations the minimal 1-norm solution is also the sparsest solution. Communications on Pure and Applied Mathematics 59(6): 797-829.
- DL Donoho (2006) Compressed sensing, IEEE Transactions on Information Theory 52(4): 1289-1306.
- EJ Candès, JK Romberg, T Tao (2016) Robust uncertainty principles: Exact signal reconstruction from highly incomplete Fourier information. IEEE Trans Inf Theory 52(8): 489-509.
- LI Rudin, S Osher, E Fatemi (1992) Nonlinear total variation-based noise removal algorithms. Physica D: Nonlinear Phenomena 60(1-4): 259-268.
- H Chen, J Tao, Y Sun, Z Ye, B Qiu, et al. (2015) Magnetic resonance image reconstruction via L0-norm minimization. 2015 IET International Conference on Biomedical Image and Signal Processing (ICBISP 2015), Beijing p. 1-6.
- Li Xu, Cewu Lu, Yi Xu, Jiaya Jia (2011) Image smoothing via L0 gradient minimization. ACM Transactions on Graphics 30(6): 174.
- Y Sun, J Tao (2014) Few views image reconstruction using alternating direction method via L0-minimization International Journal of Imaging Systems and Technology 24: 214-223.
- Wei Yu, Li Zeng (2015) l_0 gradient minimization-based image reconstruction for limited-angle computed tomography. PLOS ONE 10(7): e0130793.
- Xuan Fei, Zhihui Wei, Liang Xiao (2013) Iterative directional total variation refinement for compressive sensing image reconstruction. IEEE Signal Processing Letters 20(11): 1070-1073.
- EY Sidky, X Pan (2008) Image reconstruction in circular cone-beam computed tomography by constrained, total-variation minimization. Physics in Medicine & Biology 53: 4777-4807.
- VP Panin, GL Zeng, GT Gullberg (1999) Total variation regulated EM algorithm. IEEE Trans Nucl Sci 46(6): 2202-2210.
- GL Zeng, Y Li, A Zamyatin (2013) Iterative total-variation reconstruction versus weighted filtered-backprojection reconstruction with edge-preserving filtering. Phys Med Biol 58: 3413-3431.
- GL Zeng (2022) A projection-domain iterative algorithm for metal artifact reduction by minimizing the total-variation norm and the negative-pixel

energy. Visual Computing for Industry Biomedicine and Art 5:1.

14. LA Shepp, BF Logan (1974) The Fourier reconstruction of a head section. IEEE Transactions on Nuclear Science NS-21(3): 21-43.

ISSN: 2574-1241

DOI: 10.26717/BJSTR.2024.55.008665

Gengsheng L Zeng, Biomed J Sci & Tech Res



This work is licensed under Creative Commons Attribution 4.0 License

Submission Link: <https://biomedres.us/submit-manuscript.php>



Assets of Publishing with us

- Global archiving of articles
- Immediate, unrestricted online access
- Rigorous Peer Review Process
- Authors Retain Copyrights
- Unique DOI for all articles

<https://biomedres.us/>